

# Raman Spectroscopic Characterization of Structural Changes in Heated Whey Protein Isolate upon Soluble Complex Formation with Pectin at Near Neutral pH

Sha Zhang, Zhong Zhang, Mengshi Lin, and Bongkosh Vardhanabhuti\*

Food Science Program, Division of Food Systems and Bioengineering, University of Missouri, Columbia, Missouri 65211, United States

**ABSTRACT:** The mechanism leading to an alteration of heat aggregation of whey protein isolate (WPI) in the presence of pectin was investigated by assessing structural changes of proteins using Raman spectroscopy. WPI solutions were heated without or with pectin at 0.015–0.2 pectin to WPI weight ratios and pH 6.0–6.4. In the absence of pectin, thermal denaturation resulted in a loss of  $\alpha$ -helical structure and an increase in  $\beta$ -structure and random coils of protein. At pH 6.0 and 6.2, heat aggregation of WPI was suppressed when pectin (0.05–0.15 pectin to WPI ratios) was present as shown by a decrease in turbidity and particle size. Concomitantly, changes in the secondary structures were reduced, indicating the enhanced stability of protein structure by pectin. Raman results also revealed that  $\alpha$ -helix and  $\beta$ -sheet are dominant structures in heated WPI–pectin soluble complexes, and hydrogen bonding between biopolymers increased. The effect of pectin was pH dependent, indicating the involvement of electrostatic interaction.

**KEYWORDS:** whey proteins, pectin, heat aggregation, raman spectroscopy, turbidity

## INTRODUCTION

Complexes of proteins and polysaccharides are mostly driven by electrostatic interactions between two oppositely charged biopolymers. When proteins and polysaccharides are mixed at pH values near or below the isoelectric point (pI) of protein, a complex is formed for several protein/polysaccharide systems, such as  $\beta$ -lactoglobulin/acacia gum,  $\beta$ -lactoglobulin/pectin, soy protein isolate/acacia gum, and whey proteins/exopolysaccharide.<sup>1–5</sup> The mechanism is believed to be a pH-induced two-step structure-forming event associated with the formation of soluble and insoluble complexes.<sup>6</sup> Soluble complexes form at the critical pH first, and then, insoluble complexes and coacervates form as a consequence of the pH decreasing to near the pI of protein. However, even at the pH above the pI of protein, where both biopolymers carry a net negative charge, soluble complexes can be formed because the positively charged local domain on protein can interact with anionic polysaccharides.<sup>7,8</sup> The formation of a soluble complex at high pH can be achieved by partial or complete unfolding of protein upon heating.<sup>9</sup> During heating, some positively charged amino groups on protein will be exposed, which are available for further interaction with anionic polysaccharides and could lead to soluble complex formation.<sup>10</sup>

Proteins were partially unfolded due to an increase in charge repulsion during pH-induced complex coacervation with polysaccharides, thus leading to the conformational modifications. It was reported that the maximum loss of secondary structure in protein was obtained exactly at the pH of coacervation. Chourpa et al.<sup>4</sup> investigated the conformational changes of gliadin and globulin when forming coacervates with gum arabic at pH below the pI of protein, showing a strong increase of  $\beta$ -sheet in pea globulin and  $\alpha$ -helix in  $\alpha$ -gliadin. Schmitt et al.<sup>11</sup> found that complex coacervation of  $\beta$ -lactoglobulin and acacia gum at pH 4.2 induced the loss of

50% of the  $\alpha$ -helix content of  $\beta$ -lactoglobulin. However, Klemmer et al.<sup>5</sup> reported no significant changes in the secondary structure of pea protein when insoluble pea protein–alginate complexes formed at acidic pH. These different results were obtained from different protein–polysaccharide systems, which probably originate from the structural difference in the unfolded state of proteins and nature of the binding between protein and polysaccharides. Although it has been reported that soluble complexes could be produced during heating at near neutral pH (pH > pI of protein), much less research has been done on the molecular level to investigate the structural changes of both proteins and polysaccharides.<sup>12</sup> Studies found that the thermal stability of  $\beta$ -lactoglobulin was significantly enhanced due to the soluble complex formation with dextran sulfate at near neutral pH, but the conformational modification of proteins remained unclear.<sup>13,14</sup> Rudd et al.<sup>15</sup> investigated secondary structural changes of antithrombin in the protein–polysaccharide complex solution using vibrational circular dichroism, which indicated that the  $\beta$ -sheet secondary structure of protein underwent substantial changes during complex formation. However, these secondary structural changes have not been quantified, and more comprehensive studies are needed to quantify the structural changes of protein as a consequence of polysaccharide binding to protein at a pH well above the pI of the protein.

Accurately quantifying the secondary structural changes of protein in solution can be achieved by several methods such as nuclear magnetic resonance, circular dichroism, infrared

**Received:** August 31, 2012

**Revised:** November 5, 2012

**Accepted:** November 7, 2012

**Published:** November 7, 2012

absorption, and Raman spectroscopy. Among these methods, Raman spectroscopy is a suitable and direct technique that can provide information on primary and secondary structures of protein in both aqueous and solid samples without any pretreatment.<sup>16</sup> Raman spectroscopic analysis has been successfully employed to study the secondary structural changes of protein during thermal denaturation, heat-induced gelation, and protein–polysaccharide or protein–lipid interactions.<sup>17–24</sup>

Previous investigations on conformational modifications of protein during the protein/polysaccharide interaction were conducted at pH values where either segregative or coacervated rather than associated conditions were favored. The aim of this study is to investigate the conformational changes of whey protein isolate (WPI) upon forming associated soluble complexes with pectin at near neutral pH. WPI was chosen because it is a major food ingredient used in food products, especially beverages. Pectin was chosen since it is commonly used to stabilize dairy drinks. Low methoxyl (LM) pectin is one of the most commercially important pectins with low methyl ester and high charge density (0.6 mol negative charge/mol of monosaccharide). The effects of the pH and biopolymer ratio on thermal stability of whey proteins were investigated. Raman spectroscopy was used to measure the major conformational changes of whey proteins responsible for the formation of associated complex with pectin at near neutral pH.

## MATERIALS AND METHODS

**Chemicals.** WPI was kindly donated by Davisco Food International (BiPro, Le Sueur, MN). The WPI was constituted of 95.4% total solid, 93.1% protein, and 2.1% ash. LM pectin was a gift from CPKelco (Atlanta, GA). Hydrochloric acid was purchased from Fisher Science Education (Hanover Park, IL), and sodium hydroxide was purchased from Acros Organic (Thermo Fisher Scientific, NJ).

**Sample Preparation.** WPI stock solution (9% w/w) was prepared by dissolving the protein in Millipore water (18.2 M $\Omega$ ) with continuous stirring (at least 1 h at room temperature). Pectin stock solution (3% w/w) was prepared by dissolving pectin at 85 °C for 2 h. Both protein and pectin solutions were stored at 4 °C overnight for complete hydration. On the next day, these stock solutions were warmed to room temperature prior to mixing with each other. The WPI and pectin solutions were mixed in deionized water at the appropriate amount so that the total weight of the mixed solutions was about 90% of the final weight. The pH of the mixed solutions was adjusted from 6.0 to 6.4 using NaOH and HCl (0.1 and 0.01 N). After pH adjustment, deionized water was added to produce the designated protein and pectin concentration. Samples contained 3% w/w protein and pectin at 0 to 0.2 pectin:protein weight ratios. The pH of the final solution was checked to ensure proper pH. All samples were left at room temperature for 2 h under gentle magnetic agitation to promote complete complex formation. Then, 5 mL of each mixture was heated in a test tube at 85 °C for 15 min, cooled in ice water, and moved to room temperature for measurements.

**Turbidity Measurement.** The turbidity of the WPI–pectin soluble complex was measured using an ultraviolet–visible (UV) spectrophotometer (Shimadzu, Japan) at a wavelength of 633 nm. Samples were analyzed in disposable plastic cuvettes with a cell path length of 1.0 cm. Deionized water was used as a blank reference. All experiments were replicated at least twice.

**Particle Size Analysis.** The average particle diameter of the WPI–pectin soluble complex was measured by dynamic light scattering using the Zetasizer Nano ZS (Malvern Instruments Ltd., Worcestershire, United Kingdom) equipped with 633 nm laser and 173° detection optics. Each sample was measured by dilution with deionized water to a final protein concentration of 0.1%. The particle size was reported as the Z-average mean diameter.

**Raman Measurement.** The heated WPI–pectin soluble complex was deposited onto a gold microscope slide and dried at ambient conditions prior to Raman measurement. Raman spectra were performed using a Renishaw RM1000 Raman Spectrometer System (Gloucestershire, United Kingdom) equipped with a Leica DMLB microscope (Wetzlar, Germany). This system was equipped with a 785 nm near-infrared diode laser. During the measurement, light from the high power (maximum at 300 mW) diode laser was directed and focused onto the sample on a microscope stage through a 50 $\times$  objective. Raman scattering signals were detected by a 578  $\times$  385 pixels CCD array detector. The size of each pixel was 22  $\mu$ m  $\times$  22  $\mu$ m. The spectra were plotted as intensity (arbitrary units) versus the Raman shift in wavenumber (cm<sup>-1</sup>) with a detection range from 400 to 2000 cm<sup>-1</sup>. Duplicates were collected from three independent experiments in which six different spots were recorded on the same sample. Spectral data were collected by WiRE 1.3 software (Gloucestershire, United Kingdom) and baseline corrected and normalized according to the protein phenylalanine peak at 1003  $\pm$  1 cm<sup>-1</sup>. Protein secondary structures were determined as percentages of  $\alpha$ -helix,  $\beta$ -sheet,  $\beta$ -turn, and random coil according to Sun et al.<sup>28</sup> Spectral decompositions of the amide I band region, including normalization, derivation, curve fitting, and area calculation, were carried out using PeakFit software (Ver. 4.12, SeaSolve Software Inc. Framingham, MA). The relative amount of each component was determined from the area of the corresponding fitted band.

**Statistical Analysis.** Statistical analysis of results was performed using SPSS software (SPSS Inc., Ver. 19, Chicago, IL). A one-way analysis of variance (ANOVA) was employed to determine the statistical difference. Significant differences ( $p < 0.05$ ) between means were identified using Duncan's multiple range test.

## RESULTS AND DISCUSSION

**Turbidity.** The optimal density profiles (at 633 nm) as a function of pectin:WPI weight ratios (from 0 to 0.2) at three different pH values are shown in Figure 1. Heated protein

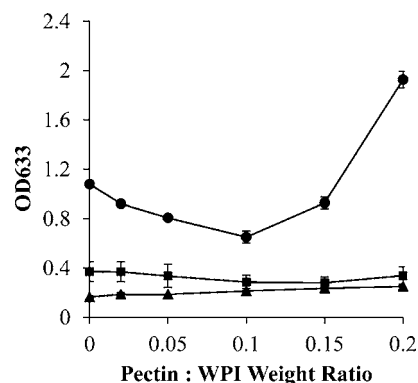


**Figure 1.** Effect of pH and biopolymer ratio on the turbidity of heated WPI and pectin: pH 6.0 (●), pH 6.2 (■), and pH 6.4 (▲).

solutions at pH 6.4 were slightly turbid, but only a small decrease in pH to 6.2 resulted in higher aggregation of WPI as indicated by an increase in turbidity. Pectin had the ability to protect WPI against aggregation at pH 6.0 and 6.2. The addition of pectin at a low concentration decreased the turbidity of the mixture, indicating that the degree of the aggregation of whey proteins was inhibited or the aggregation was modified to a different type of aggregates. At these pH values, negatively charged pectin interacted with the positively charged local domain on whey proteins, such that the protein–pectin complex formation receded protein–protein aggregation. Much was the same in the case of bovine serum albumin aggregation prevented by dextran sulfate observed by Chung et

al.<sup>25</sup> At a higher pectin concentration, the turbidity of the mixture increased dramatically as can be seen from pH 6.0. No phase separation was observed prior to heating; therefore, an increase in turbidity was probably due to cross-linking of the soluble complexes between the biopolymers during heating.<sup>14</sup>

**Particle Size.** To confirm the formation of associated complex, the particle size of the mixture was also measured, presenting as the Z-average mean diameter. The changes of particle size of whey proteins due to the presence of different concentration of pectin (Figure 2) showed the same trend as

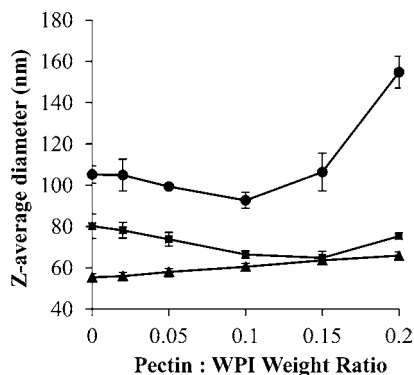


**Figure 2.** Effect of pH and biopolymer ratio on particle size of heated WPI and pectin: pH 6.0 (●), pH 6.2 (■), and pH 6.4 (▲).

the turbidity (Figure 1). At pH 6.4, the particle size of WPI aggregates slightly increased with the increased concentration of pectin. This is probably because this pH value is far away from the isoelectric point, and protein carries high negative charges that prevent pectin from binding on the protein. As a result, more pectin indicates stronger electrostatic repulsion between protein and pectin, which could result in phase separation and larger protein aggregates. At pH 6.2 and 6.0, the addition of pectin resulted in the reduced particle size of WPI aggregates, with the smallest particle size observed at pectin:WPI weight ratios of 0.15 and 0.10 at pH 6.2 and 6.0, respectively.

**Raman Spectroscopic Analysis. Comparison of Unheated and Heated Samples of Whey Proteins.** Raman spectra of native state and denatured state of whey proteins (pH 6.0) in the region of 400–2000  $\text{cm}^{-1}$  are shown in Figure 3. The frequency of major Raman bands and their tentative assignment that have been carried out according to literature references are resumed in Table 1.<sup>4,18,26</sup> The intensity difference of Raman bands between native whey proteins and denatured whey proteins mainly indicated the major protein secondary structural changes and local environmental condition changes around certain residues.<sup>26</sup>

The local environmental changes between native and denatured whey proteins were indicated by the intensity changes of the bands at 864/837, 1335, and 1449  $\text{cm}^{-1}$  (Table 2). The intensity ratio of the tyrosine (Tyr) doublet at 864 and 837  $\text{cm}^{-1}$  ( $I_{864}/I_{837}$ ), known as a good indicator of the hydrogen bonding of the phenolic hydroxyl group, has been used to reflect “buried” and “exposed” Tyr groups.<sup>18</sup> In our case, the  $I_{864}/I_{837}$  ratio of native whey proteins is 1.55, and there was a significant reduction after whey proteins were denatured ( $I_{864}/I_{837} = 1.09$ ), suggesting that some Tyr groups were buried in a hydrophobic environment, which could make a great contribution to the protein intermolecular and intramolecular hydrophobic interactions during thermal treatment.

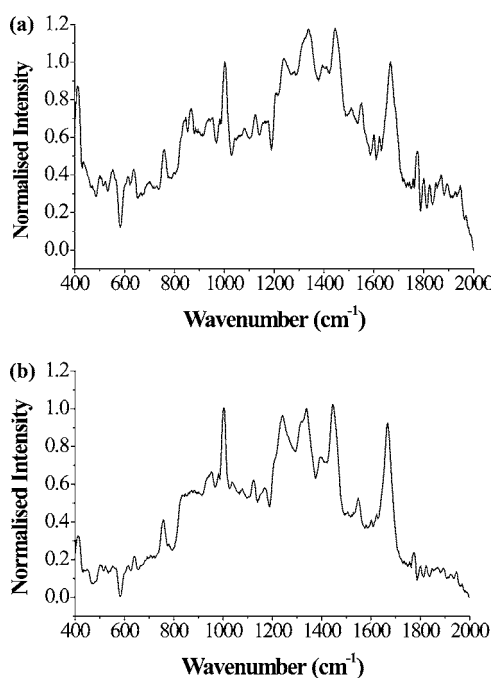


**Figure 3.** Raman spectra (400–2000  $\text{cm}^{-1}$ ) of (a) unheated and (b) heated WPI (3% w/w protein) at pH 6.0. The spectra were baselined and normalized to the phenylalanine peak at 1002  $\text{cm}^{-1}$ .

**Table 1. Tentative Assignment of Characteristic Raman Bands of Whey Protein Isolate<sup>4,18,26</sup>**

band assignment	wavenumber ( $\text{cm}^{-1}$ )
S–S stretching	507
tryptophan (Trp)	755
tyrosine (TYR) doublet	837/864
amide III ( $\alpha$ -helix)	946
phenylalanine (Phe)	1002
C–C stretching	1076
CN stretching	1112
C–C stretching	1208
amide III ( $\beta$ -sheet)	1238
amide III ( $\alpha$ -helix)	1270
CH deformation, Trp	1335
CH <sub>2</sub> or CH <sub>3</sub> bend	1449
ring stretching, Tyr	1550
amide I	1600–1700
–CH or =CH stretching	2880, 2930, 3060

Exposure of hydrophobic groups to the outer surface of protein during denaturation was evident in the present study. Denatured whey proteins showed a significant decrease in 1335  $\text{cm}^{-1}$  band assigned to C–H deformation of tryptophan (Trp), indicating the hydrophobic residues of Trp exposed to the surface of protein after heating. Another noticeable change is that denatured whey proteins showed a decrease in the intensity of the band at 1449  $\text{cm}^{-1}$  in comparison with unheated whey proteins, indicating the environmental changes around the aliphatic and hydrocarbon side chains.

It is well-known that Raman spectra could reveal secondary structural changes in protein and peptide as indicated by “amide” band envelopes, including amide I, II, and III regions. Quantitative estimation of protein secondary structure is usually obtained by fitting the amide I (1600–1700  $\text{cm}^{-1}$ ) band with theoretical profiles.<sup>4</sup> Several studies have successfully

**Table 2. Normalized Intensities of the Tyrosyl Doublet (864/837  $\text{cm}^{-1}$ ), Tryptophan Bands (1335  $\text{cm}^{-1}$ ), and  $\text{CH}_2$  or  $\text{CH}_3$  Bend (1449  $\text{cm}^{-1}$ ) of Unheated and Heated WPI at Different pH Values<sup>a</sup>**

		$I_{864}/I_{837}$ ( $\text{cm}^{-1}$ )	$I_{1335}/I_{1003}$ ( $\text{cm}^{-1}$ )	$I_{1449}/I_{1003}$ ( $\text{cm}^{-1}$ )
pH 6.0	unheated WPI	1.55 $\pm$ 0.05 d	1.50 $\pm$ 0.11 b	1.34 $\pm$ 0.06 b
	heated WPI	1.09 $\pm$ 0.02 a	1.00 $\pm$ 0.03 a	1.02 $\pm$ 0.01 a
pH 6.2	unheated WPI	1.56 $\pm$ 0.04 d	1.41 $\pm$ 0.02 b	1.30 $\pm$ 0.12 b
	heated WPI	1.21 $\pm$ 0.04 b	0.97 $\pm$ 0.05 a	1.05 $\pm$ 0.05 a
pH 6.4	unheated WPI	1.38 $\pm$ 0.05 c	1.41 $\pm$ 0.02 b	1.30 $\pm$ 0.05 b
	heated WPI	1.18 $\pm$ 0.03 ab	0.95 $\pm$ 0.14 a	1.02 $\pm$ 0.15 a

<sup>a</sup>All of the values are the means  $\pm$  standard deviations of three determinations. Different letters in the same column indicate significant difference ( $P < 0.05$ ).

deconvolved the amide I band using Gaussian or Lorentzian curve fitting to yield relative spectral contributions of the  $\alpha$ -helix,  $\beta$ -sheet,  $\beta$ -turn, and random coil to the protein secondary structures.<sup>5,27–30</sup> In this study, nine and seven Gaussian component bands were fitted to 1600–1700  $\text{cm}^{-1}$  region of unheated and heated whey proteins, respectively (Figure 4).

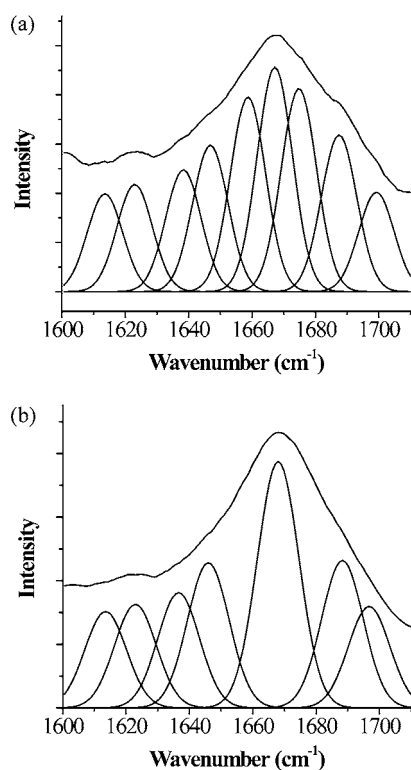


**Figure 4.** Deconvolved and curve-fitted Raman bands in the amide I band region of (a) unheated and (b) heated WPI (3% w/w protein) at pH 6.0.

The components at 1657 and 1674  $\text{cm}^{-1}$  disappeared after heating. The relative contributions of respective components were expressed as percentages of  $\alpha$ -helix,  $\beta$ -sheet,  $\beta$ -turn, and random coil conformation according to Sun et al.<sup>28</sup> (Table 3). The major feature of the amide I bands of unheated whey proteins is the  $\beta$ -sheet, as indicated by the dominance of the bands at 1667 and 1674  $\text{cm}^{-1}$ . The contribution of the  $\beta$ -sheet

decreased slightly after heating due to the disappearance of component at 1674  $\text{cm}^{-1}$ . The  $\alpha$ -helix conformation was not detected during curve fitting after heating because of the loss of the component at 1656  $\text{cm}^{-1}$ . At the expense of the helical structure, heating increased the  $\beta$ -turn and random coil fractions of whey proteins by 22.9 and 55.9%, respectively. Ngarize et al.<sup>20</sup> reported an increase in  $\beta$ -sheet in heated whey proteins. Seo et al.<sup>23</sup> reported that a loss of helical structure and formation of  $\beta$ -sheet was dominant to the conformational changes of denatured  $\beta$ -lactoglobulin. Dávila et al.<sup>31</sup> found that thermal treatment resulted in an increase in  $\beta$ -sheet content and a decrease in random coil content of plasma proteins. Vermeer and Norde<sup>32</sup> and Li et al.<sup>33</sup> described a reduction in the  $\beta$ -sheet and an increase in random coil when heating immunoglobulin. The different results obtained from this study can be explained by the presence of many different protein fractions within whey proteins as well as differences in heating conditions; thus, the overall thermal denaturation behavior can be very different from a single protein.

The Raman spectra of unheated and heated whey proteins at pH 6.2 and 6.4 were also obtained, and secondary structural changes of protein after heating showed the same trend as that at pH 6.0 (Table 3). No differences among different pH values were observed. Although different levels of protein aggregation during heat treatment were observed at these three pH values, no conformational modification could be documented from the Raman spectra.

**Conformational Changes in the Soluble WPI–Pectin Complex.** The Raman spectra of whey proteins in the presence of pectin at different biopolymer ratios and different pH values (6.0, 6.2, and 6.4) were obtained in this study. Overall conformational changes of whey proteins upon complexation with pectin were also estimated as the secondary structural modifications in amide I bands and changes of local environment around hydrophobic residues. The Raman spectra of pectin were also obtained (data not shown), which did not give significant signals as compared to protein.

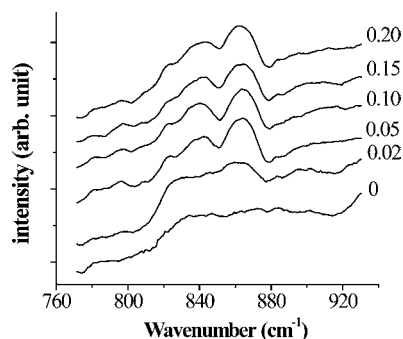
The truncated Raman spectra (770–930  $\text{cm}^{-1}$ ) of whey proteins with different pectin:WPI ratios at pH 6.0 are shown in Figure 5. The most noticeable change is the large increase in the intensity ratio of 864/837  $\text{cm}^{-1}$  doublet. As mentioned above, heating caused the burial of tyrosine residues as indicated by the decrease of the  $I_{864}/I_{837}$  ratio. However, in the presence of pectin, tyrosine was again exposed to the outer surface of protein, since the  $I_{864}/I_{837}$  ratio significantly increased with more pectin added. The most significant changes started at a certain critical pectin:WPI ratio of 0.05, which is in concordance with the results obtained from particle size measurement. The Raman spectra of whey proteins in the presence of pectin at pH 6.2 and 6.4 also showed similar results (data not shown). According to Pace et al.,<sup>34</sup> exposed tyrosine hydrogen bonds contribute favorably to protein stability even if they do not form intramolecular hydrogen bonds, and removing a partially exposed tyrosine residue on the surface of a protein causes a decrease in stability. In this study, it is possible that pectin stabilizes protein by making tyrosine residue exposed on the surface of protein during heating. On the other hand, the exposed tyrosine residue could make a great contribution to the hydrogen bonds formed between protein and pectin molecules, which might indicate the whey proteins–pectin complex formation.

Apart from the microenvironmental changes around Tyr residues, amide I bands were significantly affected by the

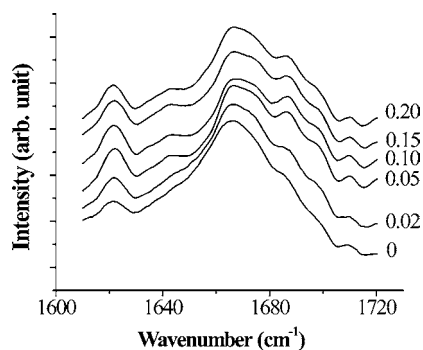
**Table 3.** Determined Frequencies of Amide I Bands, Relative Assigned Structures, and Their Contributions for Secondary Structural Contents of Unheated and Heated WPI at Different pH Values<sup>a</sup>

structure	frequency (cm <sup>-1</sup> )	structural contribution (%)					
		pH 6.0		pH 6.2		pH 6.4	
		unheated WPI	heated WPI	unheated WPI	heated WPI	unheated WPI	heated WPI
amino acid side chains	1613	7.75 ± 0.10 a	10.7 ± 0.9 c	8.88 ± 1.05 ab	10.7 ± 0.4 c	8.34 ± 0.15 a	9.91 ± 0.44 bc
$\beta$ -sheet	1623	9.27 ± 0.44 a	11.0 ± 0.3 cd	9.67 ± 0.27 ab	11.8 ± 0.4 d	9.34 ± 0.09 a	10.3 ± 0.3 bc
$\beta$ -turn	1638	9.06 ± 0.00 a	12.8 ± 1.0 b	9.33 ± 0.42 a	12.6 ± 0.4 b	9.27 ± 0.53 a	12.8 ± 1.0 b
random coil	1646	10.5 ± 0.5 a	16.4 ± 1.7 b	10.7 ± 0.7 a	16.7 ± 1.2 b	10.3 ± 0.6 a	17.2 ± 1.6 b
$\alpha$ -helix	1657	13.1 ± 1.2 a		12.6 ± 1.2 a		12.8 ± 1.4 a	
$\beta$ -sheet	1667	15.5 ± 0.2 a	25.2 ± 0.8 b	15.4 ± 0.9 a	24.2 ± 0.5 b	18.5 ± 3.9 a	23.6 ± 1.8 b
	1674	14.2 ± 0.2 a		14.1 ± 0.4 a		13.8 ± 0.6 a	
$\beta$ -turn	1687	11.8 ± 0.5 ab	14.5 ± 1.3 bc	10.3 ± 2.1 a	14.7 ± 0.4 bc	10.6 ± 0.4 a	16.0 ± 2.0 c
	1698	8.68 ± 0.41 a	9.30 ± 1.80 a	9.00 ± 0.18 a	9.23 ± 0.18 a	9.14 ± 0.69 a	10.1 ± 1.8 a
total $\alpha$ -helix		13.1 ± 1.3 a		12.6 ± 1.2 a		12.8 ± 1.4 a	
total $\beta$ -sheet		39.0 ± 0.8 a	36.3 ± 0.5 b	39.2 ± 1.0 a	36.0 ± 0.1 b	41.6 ± 3.4 a	33.9 ± 1.6 b
total $\beta$ -turn		29.6 ± 0.9 a	36.6 ± 2.1 b	28.6 ± 1.9 a	36.5 ± 1.0 b	27.0 ± 1.6 a	39.0 ± 2.8 b
total random coil		10.5 ± 0.5 a	16.4 ± 1.7 b	10.7 ± 0.7 a	16.7 ± 1.3 b	10.3 ± 0.6 a	17.2 ± 1.6 b
other		7.75 ± 0.10 a	10.7 ± 0.9 c	8.88 ± 1.0 a	10.7 ± 0.4 c	8.34 ± 0.15 a	9.91 ± 0.44 bc

<sup>a</sup>All of the values are the means  $\pm$  standard deviations of three determinations. Different letters in the same row indicate significant differences ( $P < 0.05$ ).

**Figure 5.** Raman spectra in the 770–930 cm<sup>-1</sup> region of the WPI–pectin complex formed at pH 6.0 and different biopolymer ratios.

presence of pectin at different pH values. Figure 6 showed the truncated Raman spectra (1610–1720 cm<sup>-1</sup>) of whey proteins

**Figure 6.** Raman spectra in the 1610–1720 cm<sup>-1</sup> region of the WPI–pectin complex formed at pH 6.0 and different biopolymer ratios.

at pH 6.0 with different WPI:pectin ratios. The deconvolution and curve fitting of amide I bands were obtained, and the corresponding results of the contribution of four major conformation-related components to main protein secondary structure are displayed in Table 4. The most noticeable structural change was the reoccurrence of  $\alpha$ -helix at pH 6.0 and

6.2 having pectin:WPI ratios above 0.05. At these pH values, a low pectin concentration (pectin:WPI ratio = 0.02) was not significant enough to induce conformational modification of whey proteins, while a higher pectin concentration resulted in increases in  $\alpha$ -helix and  $\beta$ -sheet accompanied by reduction in  $\beta$ -turn and random coil structures. Although thermal treatment resulted in a loss of  $\alpha$ -helix and increased random coils, a small amount of pectin binding to protein had the ability against these conformational changes, suggesting that whey proteins were stabilized by the formation of whey proteins–pectin complex. The  $\beta$ -sheet structure is characterized by a relatively large surface area that provides opportunities for the formation of hydrogen bonds.<sup>4</sup> In the presence of pectin, the increased  $\beta$ -sheet structure indicates an enhanced hydrogen bonding between protein and pectin. The pectin:WPI ratio at 0.05 also seemed to be the critical ratio prior to significant secondary structural modification. At pH 6.4, whey proteins were less influenced by the presence of pectin despite the concentration studied, which is consistent with the turbidity and particle size changes (Figures 1 and 2). It is possible that, at optimal pectin concentration and optimal electrostatic balance, pectin stabilizes protein and/or forms soluble complexes with WPI and the resulting structures dominant in  $\alpha$ -helix and  $\beta$ -sheet structures. Because these effects are observed at pH 6.0 and 6.2, it is likely that the electrostatic interactions between biopolymers, in addition to hydrogen bonding, are responsible for the formation of soluble complexes.

Several studies have reported the changes in protein secondary structure upon complex coacervates formation with polysaccharides. Girard et al.<sup>1</sup> investigated the  $\beta$ -lactoglobulin–pectin binding at pH 4 using isothermal titration calorimetry. Because of the limitation of enthalpic analysis, the authors suggested that more studies were needed to dissociate enthalpic contributions from conformational changes. Chourpa et al.<sup>4</sup> reported that pH 2.75 and 3.0 were the specific pH conditions for optimal complex coacervation of  $\alpha$ -gliadin and globulin with gum Arabic, respectively, and Raman analysis implied that the protein–gum complexes are mainly  $\beta$ -sheets in globulin and  $\alpha$ -helix in  $\alpha$ -gliadin. Klemmer et al.<sup>5</sup> showed no significant changes in secondary structure composition of pea protein

**Table 4. Relative Contributions of Four Major Conformation-Related Components (Curve Fitting Made as for Figure 4) in Amide I Band of Unheated WPI, Heated WPI, and WPI–Pectin Complex at pH 6.0, 6.2, and 6.4<sup>a</sup>**

structure	pH	structural distribution (%)						
		unheated	pectin:WPI weight ratio					0.20
			0.00	0.02	0.05	0.10	0.15	
$\alpha$ -helix	6.0	13.1 ± 1.3 a			10.9 ± 0.4 a	11.7 ± 1.6 a	11.6 ± 1.2 a	11.2 ± 0.3 a
	6.2	12.6 ± 1.2 a			11.5 ± 0.3 a	11.1 ± 0.9 a	11.1 ± 0.0 a	12.8 ± 1.4 a
	6.4	12.8 ± 1.4 a						
$\beta$ -sheet	6.0	39.0 ± 0.8 cd	36.3 ± 0.5 ab	36.8 ± 0.1 bc	40.8 ± 0.9 d	40.8 ± 0.8 d	39.9 ± 1.0 d	40.7 ± 0.0 d
	6.2	39.2 ± 1.0 cd	36.0 ± 0.1 ab	36.3 ± 0.6 ab	39.9 ± 0.6 d	40.2 ± 0.1 d	40.7 ± 0.4 d	44.2 ± 1.0 e
	6.4	41.6 ± 3.4 d	33.9 ± 1.6 a	36.9 ± 0.7 bc	35.6 ± 0.7 ab	35.5 ± 0.6 ab	34.1 ± 1.7 a	34.8 ± 0.9 ab
$\beta$ -turn	6.0	29.6 ± 0.8 bc	36.6 ± 2.1 fg	34.8 ± 1.3 ef	31.4 ± 0.7 cde	30.3 ± 2.6 bcd	30.5 ± 1.9 bcd	31.1 ± 0.1 cde
	6.2	28.6 ± 1.9 bc	36.5 ± 1.0 fg	37.7 ± 0.4 fg	30.5 ± 1.1 bcd	31.3 ± 1.2 cde	30.7 ± 0.2 bcd	23.1 ± 0.7 a
	6.4	27.0 ± 1.6 b	39.0 ± 2.8 g	34.0 ± 0.6 def	36.5 ± 0.4 fg	37.3 ± 3.7 fg	36.7 ± 2.9 fg	39.3 ± 1.2 g
random coil	6.0	10.5 ± 0.5 a	16.4 ± 1.7 cde	17.5 ± 1.4 de	9.55 ± 0.24 a	9.71 ± 0.1 a	9.93 ± 0.08 a	11.2 ± 0.0 a
	6.2	10.7 ± 0.7 a	16.7 ± 1.3 cde	15.2 ± 0.1 bc	10.0 ± 0.5 a	9.88 ± 0.35 a	9.82 ± 0.01 a	12.4 ± 0.5 a
	6.4	10.3 ± 0.5 a	17.2 ± 1.6 cde	18.2 ± 0.3 e	15.5 ± 0.1 bcd	15.9 ± 2.2 cd	16.2 ± 0.7 cde	13.8 ± 0.5 b

<sup>a</sup>All of the values are the means ± standard deviations of three determinations. Different letters under the same structure indicate significant differences ( $P < 0.05$ ).

upon the complex coacervation of alginate polysaccharides. Despite the different results obtained in these studies, the insoluble protein–polysaccharide complexes were pH-induced at pH near or below the pI of protein and at a polysaccharide:protein ratio around 0.5 to 1 at room temperature. In this study, much less polysaccharide was used to produce the soluble complex at near neutral pH by heating the mixture of the two biopolymers. During heating, protein unfolds, which offers a greater chance for pectin to bind on the positively charged domain on protein than when protein is in its native state.

**Possible Mechanisms of Soluble Complex Formation.** Concerning electrostatic repulsion between both negatively charged protein and pectin at a pH away from isoelectric point, the initial hypothesis is that there should be an optimal pH and biopolymer ratio that provide balanced electrostatic repulsion and attraction, favoring the formation of soluble protein–pectin complex. At higher pH, microscopic phase separation would occur, which leads to disassociation of the complex. The results obtained in this study confirmed this hypothesis. At a pH value above pI but below 6.4, pectin is able to bind to the positively charged patches on whey proteins and rather favorable to form associated whey proteins–pectin complexes. Only a small increase in pH results in much less interaction between whey proteins and pectin.

The mechanism of whey proteins and pectin interaction at near neutral pH can be carefully detailed from Raman investigations carried out in the 400–2000  $\text{cm}^{-1}$  region. Whey protein denaturation results in the loss of  $\alpha$ -helix and a concomitant formation of  $\beta$ -structure of unordered coil. By adding an appropriate amount of pectin to whey protein solution, less modification of secondary structure is detected. On the other hand, significant increases in the  $I_{864}/I_{837}$  ratio and  $\beta$ -sheet structure indicate the importance of electrostatic interaction and hydrogen bonding for protein–pectin interactions. In addition, the pectin concentration plays an important role in optimal complex formation at near neutral pH. Above the optimal biopolymer ratio, a higher amount of pectin could cause either microscopic phase separation or cross-linking between biopolymers.

The results described in this study provide additional evidence to previous analyses of polysaccharide and protein interactions at near neutral pH and its effect on protein heat stability. It has been shown that the heat stability of protein enhanced by forming a soluble complex with polysaccharide is driven by the electrostatic interactions between the two biopolymers. Combined with this study, we can conclude that the effect of polysaccharide is mainly due to its ability to stabilize the secondary structures and further alter the heat aggregation of protein.

## AUTHOR INFORMATION

### Corresponding Author

\*Tel: 573-8821374. Fax: 573-8847964. E-mail: VardhanabhutiB@missouri.edu.

### Notes

The authors declare no competing financial interest.

## ACKNOWLEDGMENTS

We thank Davisco Foods International Inc. for providing WPI and CPKelco for providing pectin.

## REFERENCES

- (1) Girard, M.; Turgeon, S. L.; Gauthier, S. F. Thermodynamic parameters of  $\beta$ -lactoglobulin-pectin complexes assessed by isothermal titration calorimetry. *J. Agric. Food Chem.* **2003**, *51*, 4450–4455.
- (2) Weinbreck, F.; Nieuwenhuijse, H.; Robijn, G. W.; de Kruijff, C. G. Complex formation of whey proteins: exocellular polysaccharide EPS B40. *Langmuir* **2003**, *19*, 9404–9410.
- (3) Mekhloufi, G.; Sanchez, C.; Renard, D.; Guillemin, S.; Hardy, J. pH-induced structural transitions during complexation and coacervation of  $\beta$ -lactoglobulin and acacia gum. *Langmuir* **2005**, *21*, 386–394.
- (4) Chourpa, I.; Ducel, V.; Richard, J.; Dubois, P.; Boury, F. Conformational modifications of  $\alpha$  gliadin and globulin proteins upon complex coacervates formation with gum arabic as studied by raman microspectroscopy. *Biomacromolecules* **2006**, *7*, 2616–2623.
- (5) Klemmer, K.; Waldner, L.; Stone, A.; Low, N.; Nickerson, M. Complex coacervation of pea protein isolate and alginate polysaccharides. *Food Chem.* **2012**, *130*, 710–715.
- (6) Turgeon, S.; Schmitt, C.; Sanchez, C. Protein-polysaccharide complexes and coacervates. *Curr. Opin. Colloid Interface Sci.* **2007**, *12*, 166–178.

- (7) Girard, M.; Turgeon, S. L.; Gauthier, S. F. Interbiopolymer complexing between  $\beta$ -lactoglobulin and low- and high-methylated pectin measured by potentiometric titration and ultrafiltration. *Food Hydrocolloids* **2002**, *16*, 585–591.
- (8) Tokle, T.; Lesmes, U.; McClements, D. J. Impact of electrostatic deposition of anionic polysaccharides on the stability of oil droplets coated by lactoferrin. *J. Agric. Food Chem.* **2010**, *58*, 9825–9832.
- (9) Gentès, M. C.; St-Gelais, D.; Turgeon, S. L. Stabilization of Whey Protein Isolate–Pectin Complexes by Heat. *J. Agric. Food Chem.* **2010**, *58*, 7051–7058.
- (10) De la Fuente, M.; Hemar, Y.; Singh, H. Influence of  $\kappa$ -carrageenan on the aggregation behaviour of proteins in heated whey protein isolate solutions. *Food Chem.* **2004**, *86*, 1–9.
- (11) Schmitt, C.; Sanchez, C.; Despond, S.; Renard, D.; Robert, P.; Hardy, J. Structural modification of  $\beta$ -lactoglobulin as induced by complex coacervation with acacia gum. In *Food Colloids Fundamentals of Formulation*; Dickinson, E., Miller, R., Eds.; The Royal Society of Chemistry: Cambridge, United Kingdom, 2001; pp 323–331.
- (12) Dickinson, E. Stability and rheological implications of electrostatic milk protein-polysaccharide interactions. *Trends Food Sci Technol.* **1998**, *9*, 347–354.
- (13) Vardhanabhuti, B.; Allen Foegeding, E. Effects of dextran sulfate, NaCl, and initial protein concentration on thermal stability of  $\beta$ -lactoglobulin and  $\alpha$ -lactalbumin at neutral pH. *Food Hydrocolloids* **2008**, *22*, 752–762.
- (14) Vardhanabhuti, B.; Yucel, U.; Coupland, J. N.; Foegeding, E. A. Interactions between  $\beta$ -lactoglobulin and dextran sulfate at near neutral pH and their effect on thermal stability. *Food Hydrocolloids* **2009**, *23*, 1511–1520.
- (15) Rudd, T. R.; Nichols, R. J.; Yates, E. A. Selective detection of protein secondary structural changes in solution protein-polysaccharide complexes using vibrational circular dichroism (VCD). *J. Am. Chem. Soc.* **2008**, *130*, 2138–2139.
- (16) Li-Chan, E. The applications of Raman spectroscopy in food science. *Trends Food Sci. Technol.* **1996**, *7*, 361–370.
- (17) Linlaud, N.; Ferrer, E.; Puppo, M. C.; Ferrero, C. Hydrocolloid interaction with water, protein, and starch in wheat dough. *J. Agric. Food Chem.* **2010**, *59*, 713–719.
- (18) Nonaka, M.; Li-Chan, E.; Nakai, S. Raman spectroscopic study of thermally induced gelation of whey proteins. *J. Agric. Food Chem.* **1993**, *41*, 1176–1181.
- (19) Alizadeh-Pasdar, N.; Nakai, S.; Li-Chan, E. C. Y. Principal component similarity analysis of Raman spectra to study the effects of pH, heating, and  $\kappa$ -carrageenan on whey protein structure. *J. Agric. Food Chem.* **2002**, *50*, 6042–6052.
- (20) Ngarize, S.; Adams, A.; Howell, N. K. Studies on egg albumen and whey protein interactions by FT-Raman spectroscopy and rheology. *Food Hydrocolloids* **2004**, *18*, 49–59.
- (21) Meng, G.; Chan, J. C. K.; Rousseau, D.; Li-Chan, E. C. Y. Study of protein-lipid interactions at the bovine serum albumin/oil interface by Raman microspectroscopy. *J. Agric. Food Chem.* **2005**, *53*, 845–852.
- (22) Ngarize, S.; Adams, A.; Howell, N. A comparative study of heat and high pressure induced gels of whey and egg albumen proteins and their binary mixtures. *Food Hydrocolloids* **2005**, *19*, 984–996.
- (23) Seo, J. A.; Hédoux, A.; Guinet, Y.; Paccou, L.; Affouard, F.; Lerbet, A.; Descamps, M. Thermal Denaturation of Beta-Lactoglobulin and Stabilization Mechanism by Trehalose Analyzed from Raman Spectroscopy Investigations. *J. Phys. Chem. B* **2010**, *114*, 6675–6684.
- (24) Ikeda, S. Heat-induced gelation of whey proteins observed by rheology, atomic force microscopy, and Raman scattering spectroscopy. *Food Hydrocolloids* **2003**, *17*, 399–406.
- (25) Chung, K.; Kim, J.; Cho, B. K.; Ko, B. J.; Hwang, B. Y.; Kim, B. G. How does dextran sulfate prevent heat induced aggregation of protein?: The mechanism and its limitation as aggregation inhibitor. *Biochim. Biophys. Acta, Proteins Proteomics* **2007**, *1774*, 249–257.
- (26) Li-Chan, E. C. Y. Vibrational spectroscopy applied to the study of milk proteins. *Lait* **2007**, *87*, 443–458.
- (27) Maiti, N. C.; Apetri, M. M.; Zagorski, M. G.; Carey, P. R.; Anderson, V. E. Raman spectroscopic characterization of secondary structure in natively unfolded proteins:  $\alpha$ -Synuclein. *J. Am. Chem. Soc.* **2004**, *126*, 2399–2408.
- (28) Sun, W.; Zhao, Q.; Zhao, M.; Yang, B.; Cui, C.; Ren, J. Structural evaluation of myofibrillar proteins during processing of Cantonese sausage by Raman spectroscopy. *J. Agric. Food Chem.* **2011**, *59*, 11070–11077.
- (29) Susi, H.; Byler, D. M. Fourier deconvolution of the amide I Raman band of proteins as related to conformation. *Appl. Spectrosc.* **1988**, *42*, 819–826.
- (30) Liang, M.; Chen, V. Y. T.; Chen, H. L.; Chen, W. A simple and direct isolation of whey components from raw milk by gel filtration chromatography and structural characterization by Fourier transform Raman spectroscopy. *Talanta* **2006**, *69*, 1269–1277.
- (31) Dávila, E.; Parés, D.; Howell, N. K. Fourier transform Raman spectroscopy study of heat-induced gelation of plasma proteins as influenced by pH. *J. Agric. Food Chem.* **2006**, *54*, 7890–7897.
- (32) Vermeer, A. W. P.; Norde, W. The thermal stability of immunoglobulin: unfolding and aggregation of a multi-domain protein. *Biophys. J.* **2000**, *78*, 394–404.
- (33) Li, S. Q.; Bomser, J. A.; Zhang, Q. H. Effects of pulsed electric fields and heat treatment on stability and secondary structure of bovine immunoglobulin G. *J. Agric. Food Chem.* **2005**, *53*, 663–670.
- (34) Pace, C. N.; Horn, G.; Hebert, E. J.; Bechert, J.; Shaw, K.; Urbanikova, L.; Scholtz, J. M.; Sevcik, J. Tyrosine hydrogen bonds make a large contribution to protein stability. *J. Mol. Biol.* **2001**, *312*, 393–404.